Nuclear Materials and Energy 3–4 (2015) 17–21

Contents lists available at ScienceDirect

Nuclear Materials and Energy

journal homepage: www.elsevier.com/locate/nme

# Microstructure and mechanical properties of V–Me(Cr,W)–Zr alloys as a function of their chemical–thermal treatment modes

V.M. Chernov[a,b,*], M.M. Potapenko[a], V.A. Drobyshev[a], M.V. Kravtsova[a], A.N. Tyumentsev[c,d,e], S.V. Ovchinnikov[c,d], I.A. Ditenberg[c,d], Y.P. Pinzhin[c,d,e], A.D. Korotaev[c,d,e], I.V. Smirnov[d,e], K.V. Grinyaev[c,d,e], I.I. Sukhanov[e]

[a] A.A. Bochvar High Technology Research Institute of Inorganic Materials, 123098 Moscow, Russia
[b] National Research Nuclear University MEPhI, 115409 Moscow, Russia
[c] Institute of Strength Physics and Materials Science, Siberian Branch of the Russian Academy of Sciences, 634021 Tomsk, Russia
[d] V.D. Kuznetsov Siberian Physical-Technical Institute at Tomsk State University, 630050 Tomsk, Russia
[e] Tomsk State University, 634050 Tomsk, Russia

ARTICLE INFO

*Article history:*
Received 11 February 2015
Revised 28 April 2015
Accepted 30 April 2015
Available online 5 July 2015

*Key words:*
Vanadium alloys
V–Me(Cr,W)–Zr alloys
Thermochemical treatment
Internal oxidation
Thermomechanical treatment
Electron microscopy
Microstructure
Dispersion hardening

ABSTRACT

Formation of regularities of the nanometric oxide precipitates and defect microstructure in vanadium-based low activation alloys V–Cr–Zr–(C,N,O) and V–Cr–W–Zr–(C,N,O) as a function of the regimes of their thermo-chemical treatment was investigated. Several methods of internal oxidation which provide formation of the nanosized $ZrO_2$ particles of controllable dispersion, ensure the nanometric size of the heterophase structure to be maintained up to the temperatures as high as 1300–1400 °C, and allow the recrystallization temperature to be increased up to ≥1400 °C were proposed. Formation of such microstructure contributes to dispersion- and substructural hardening and results in more than twofold increase in the yield stress of these alloys both at room and elevated (800 °C) temperatures, compared to the conventional thermo-mechanical treatment.



## 1. Introduction

Low-activated vanadium alloys of V–Ti–Cr system (V–4Ti–4Cr is the best reference alloy) as the structural materials for cores of fusion and fission (fast) nuclear reactors are considered [1–4]. New compositions of vanadium low-activated alloys of V–Me(Cr, W)–Zr-C system demonstrate good prospects [5]. This prospect is related to the possibility of modifying these alloys' heterophase structure (a significant increase in the dispersity and the uniformity of the spatial distribution of the zirconium carbide particles—ZrC) by methods of thermomechanical treatment (TMT). According to [5], the significant increase of short-term high temperature ($T$ = 800 °C) strengthening (by 50%) and the recrystallization temperature (approximately by 100–200 °C) can be achieved using TMT methods in V–Me(Cr, W)–Zr–C alloys compared to V–4Ti–4Cr alloys due to higher volume fraction and thermal stability of the superfine non-metallic (ZrC) phase particles. Significantly higher increase of the thermal stability of the nanostructured heterophase structure, the recrystallization temperature and characteristics of the long-term high-temperature strength of the vanadium alloys can be achieved with the use of chemical–thermal treatment (CTT) [6,7].

High solubility and diffusion mobility of the oxygen are typical for vanadium alloys at comparatively low temperatures ($T \leq 0.4\ T_{melt}$, $T_{melt}$ is the melting temperature), which allow one to realize the non-equilibrium internal oxidation (IO) in Zr-bearing vanadium alloys, which gives rise to formation of $ZrO_2$ particles simultaneously in the entire volume of the specimens under the conditions of highly oversaturated non-equilibrium V–Zr–O solid solutions. It should be noted that as a result of slight changes in the conditions of nucleation and growth of a new phase in case of a deeper IO, it becomes possible to form the uniform distribution of $ZrO_2$ particles with an approximately unlimited degree of size fineness (particle's sizes < 10 nm).

High negative value of the thermodynamic potential of $ZrO_2$ phase formation ensures a high thermal stability of the fine-dispersed heterophase state and the possibility of an effective control over the coagulation rate of these particles by varying the oxygen concentration in V–Me(Cr,W)–Zr alloys. The possibility of forming of the

* Corresponding author at: A.A. Bochvar High Technology Research Institute of Inorganic Materials, 123098 Moscow, Russia. Tel.: +7(499)190 3605; fax: +7(499)196 4168.
*E-mail address:* VMChernov@bochvar.ru, soptimizmom@mail.ru (V.M. Chernov).

http://dx.doi.org/10.1016/j.nme.2015.04.001

fine-dispersed heterophase states (e.g., V–$ZrO_2$) remaining stable at up to $T \approx 0.8\ T_{melt}$ was shown in [6,7]. These states suppress the recrystallization processes in specimens up to the temperature as high as 0.8 $T_{melt}$ under conditions of the IO of the specimens with a high defect density.

In this work we present the results of an effective dispersion hardening of V–Me(Cr,W)–Zr alloys with nanosized $ZrO_2$ particles using the TCT by the IO method.

## 2. Materials and experimental procedure

The investigation was carried out with the use of the vanadium low-activated alloys V–8.75Cr–0.14W–1.17Zr–0.01C–0.02O–0.01N (wt. %) and V–4.23Cr–7.56W–1.69Zr-–0.02C–0.02O–0.01N (Alloy 1 and Alloy 2, respectively) manufactured in A.A. Bochvar Institute. Chromium and tungsten alloying provides the opportunity of values variation of the solid solution strengthening.

The initial specimens of the studied alloys represented the sheets of the 1 mm thick made using traditional thermomechanical treatment (TMT-I), similar to the treatment presented in [8], which involves the following stages:

1. Homogenizing vacuum annealing of the ingot at the temperature of 1300 °C for 8 h.
2. Extrusion (pressing) at the elevated temperature.
3. Conclusive rolling and upsetting cycles at room temperature with intermediate vacuum annealing at $T = (950–1000)$ °C.
4. Conclusive stabilizing vacuum annealing at the temperature of 1000 °C for 1 h.

The specimens were heat-treated in the vacuum furnaces at $\approx 3 \times 10^{-3}$ Pa. The structural studies were performed by the methods of optical metallography at Olympus GX-71 and NEOPHOT-21 microscopes and by transmission electron microscopy using Philips CM-30 and CM-12 microscopes at the accelerating voltages of 300 and 120 kV, respectively. The mechanical tests by the method of dynamic tensile loading were performed in vacuum at $\approx 3 \times 10^{-3}$ Pa at the strain rate $\dot{\varepsilon} \approx 2 \times 10^{-3}\ s^{-1}$ using flat specimens shaped as dumbbells with the gage section of 13 mm × 2 mm × 0.8 mm (at least 3 specimens for each temperature and condition).

## 3. The method of diffusion doping of vanadium alloys by oxygen

The stability of the oxidative medium on the stage of the alloys' saturation by the oxygen plays an important role in designing of the practical modes of controlled diffusion doping of vanadium alloys by oxygen. Conventionally, such saturation is performed in degrading oxides medium [6]. However, the existing practices of the IO of heat-resistant alloys demonstrate that application of this method is complicated by the necessity of removing of the extraneous impurities from these oxides, in particular, from volatile compounds containing oxygen (e.g., lower oxides).

One of the possible ways to stabilize the velocity of the diffusion-assisted saturation of the specimens with oxygen is to apply the diffusion doping via heat treatment in air followed by the transfer of the oxygen from the surface scale into the bulk of the specimens by high-temperature vacuum annealing. In this work, the above-described process via the modes of diffusion doping with oxygen is used. It was shown that these operating modes ensure a sufficiently high stability of the oxidation velocity. The technological process is simple and would not involve any additional costs associated with designing of the special equipment to perform the IO and to monitor the oxidation medium.

To achieve high thermal stability of the oxide phase, the concentration of oxygen in the internally oxidized specimens ($C_O$) should be higher than the concentration required for complete binding of the oxide-forming element during formation of the oxides of the corresponding stoichiometric compositions [6,7]. To achieve this goal in the studied alloys, the oxygen concentration should be $C_O > 1.3$ at.% (Alloy 1) and $C_O > 1.9$ at.% (Alloy 2) under corresponding zirconium concentrations and formation of $ZrO_2$ oxides. In this work, relying on these data and aiming at the use of different values of the volume fraction and thermal stability (coagulation rate) of the oxide phase, we performed two types of chemical–thermal treatment (CTT) procedures for each of alloys.

CTT-I—diffusion doping modes to achieve oxygen concentrations of $C_O \approx 1.4$ and 2.1 at.% in Alloy 1 and Alloy 2, respectively, in order to ensure high thermal stability of nanosized $ZrO_2$ particles and, hence, a considerable increase in the alloy's recrystallization temperature;

CTT-II—diffusion doping modes corresponding to twice lower oxygen concentrations ($C_O \approx 0.7$ and 1.2 at.% in Alloy 1 and Alloy 2, respectively) and volume fractions of the oxide particles, and much lower thermal stability of the heterophase nanostructured state, compared to CTT-I.

The concentration of the oxygen absorbed by the specimens was measured by weighing using the analytical laboratory scales. For the specimens used in this experiment, the oxygen-concentration measurement error was $\pm 3 \times 10^{-3}$ at.%. The annealing after the IO of the specimens was performed at $T = 1000$ °C for 1 h.

## 4. Experimental results

Before a CTT, the heterophase structure of both studied alloys was characterized by the presence of oxicarbonitride zirconium particles with a high content of carbon (ZrC particles) with the sizes from ≈0.1 to 0.3 μm (Fig. 1a). These particles retard recrystallization of the alloys, so the fine-crystalline or polygonal structure becomes formed after TMT-I (grain and polygon sizes from ≈1 to ≈3 μm) characterized by high dislocation density.

Two types of $ZrO_2$ particles are observed in the electron microscopy replicas with the extracted second-phase precipitates (Fig. 1b and c) after the IO and the finishing annealing at 1000 °C for 1 h, irrespective of the CTT regime:

1. Comparatively large particles (Fig. 1b) with size (tenths of a micrometer) and shape similar to the initial carbide particles (Fig. 1a).
2. $ZrO_2$ particles with size of a few nanometers (Fig. 1c).

According to the mechanisms of low-temperature IO of two-phase bcc alloys (containing carbide particles) [6], formation of the oxides occurs via oxidation of the initial carbide particles due to a low rate of carbide dissolution in the reaction zone of IO (compared to oxygen saturation rate). Since the shape and features of the spatial distribution of comparatively large particles of the first type are similar to ZrC particles in the initial (before the IO) state, it is clear that these particles are produced during the IO via the above-mentioned mechanism. The finer particles of the second type are formed via precipitation from a solid solution, their fine size being determined by low mobility of zirconium atoms.

As follows from the electron diffraction patterns (Fig. 1b and c), the particles of different sizes have different types of the crystal lattice: monoclinic (the particle size are tenths of a micron, Fig. 1b) and face-centered cubic (fcc) or face-centered tetragonal (fct) lattices (for the particle sizes of a few nanometers, Fig. 1c). According to [6], these differences result from the changes in the type of the crystal lattice (monoclinic → orthorhombic → fct → fcc) in the course of particle's size reduction.

Investigation of the thermal stability of microstructure indicates a considerable increase in the recrystallization temperature after the IO (Fig. 2). In both alloys, the temperature of the onset of collective recrystallization corresponds to that of the carbide phase dissolution and is found to be ≈1300 °C, the grain size after a one-hour

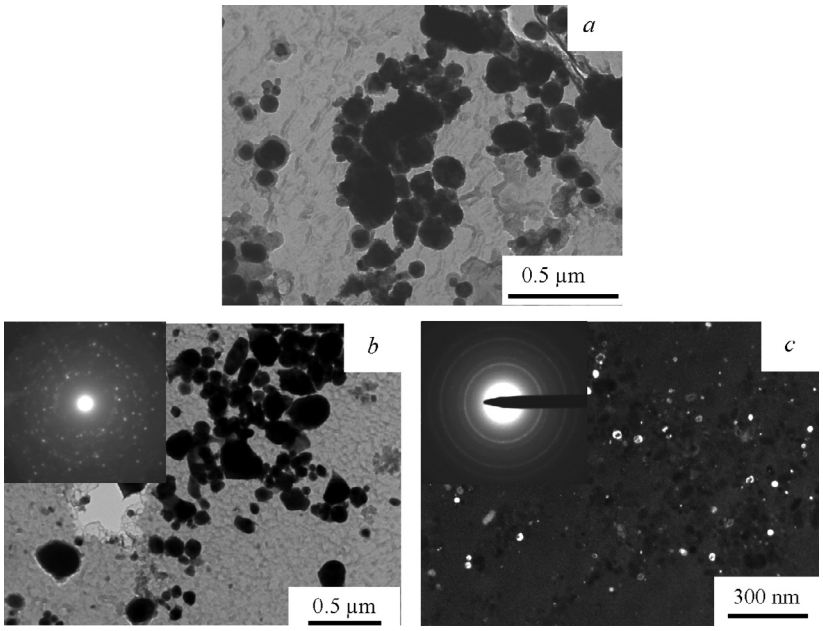


**Fig. 1.** Particles of ZrC in the initial state (a) and $ZrO_2$ (b) and (c) in their monoclinic (b) and fcc- or fct-modifications (c) in Alloy 2 after CTT-I. The replicas exhibit extracted $ZrO_2$ particles.

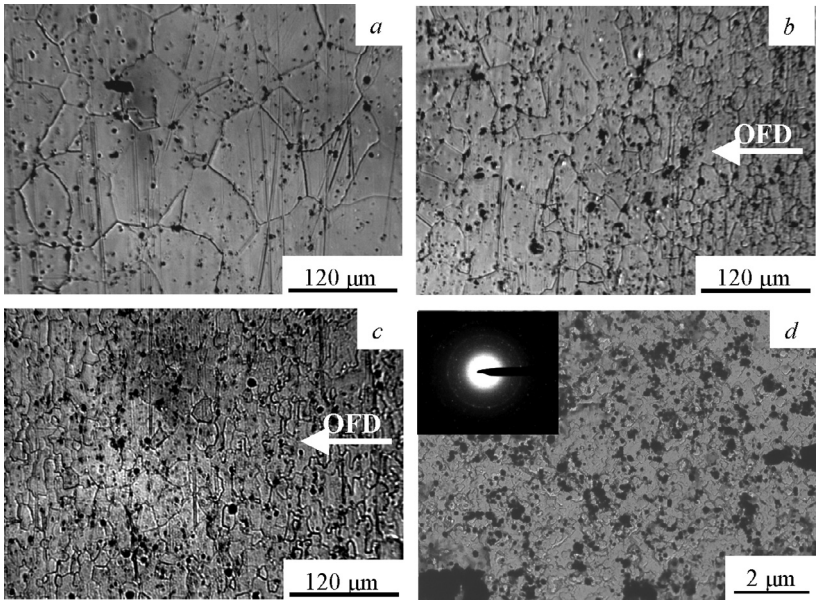


**Fig. 2.** Microstructure of the specimen of Alloy 2 after annealing at 1400 °C for 1 h: in the initial state (TMT-I prior to CTT) (a), after CTT-II (b) and after CTT-I (c). Optical metallography. Metallographic cross-sections are perpendicular to the plane of the internal oxidation front. OFD—oxidation front direction. (d) $ZrO_2$ particles after CTT-I and annealing at 1400 °C for 1 h. Transmission electron microscopy.

annealing at the temperatures of 1300 °C and 1400 °C is about 50 and 100 μm, respectively. The recrystallization temperature in the internally oxidized specimens grows by a few hundred degrees. Its finite values and the intensity of the primary recrystallization are determined by the thermal stability of the highly dispersed oxide phase, which as shown above depends on the concentration of oxygen in the alloy.

Fig. 2 illustrates an example of such dependence. In case of Alloy 2, with its zirconium concentration $C_{Zr} \approx 0.95$ at.%, the internally oxidized specimen with $C_O \approx 1.2$ at.% in the course of formation of $ZrO_2$ particles after annealing at $T = 1400$ °C contains over 0.35 at.% Zr in solid solution. According to [7], if a phase diagram is not available, the values of the equilibrium solubility of zirconium and oxygen in vanadium ($C_{Zr}^{eq}$ and $C_O^{eq}$) can be estimated from the following formula:

$$\left(C_{Zr}^{eq}\gamma_{Zr}\right) \times \left(C_O^{eq}\gamma_O\right)^2 \approx \exp\left(\Delta G^0_{ZrO_2}/R_0T\right) \quad (1)$$

where $\gamma_{Zr} \sim 1$ and $\gamma_O \approx \exp(\Delta G^0_{VO}/R_0T)$ are the coefficients of activity of these elements; $\Delta G^0_{ZrO2}$ and $\Delta G^0_{VO}$ are the formation energies of the corresponding oxides. With $\Delta G^0_{ZrO2} \approx -(1000–1100)$ kJ/mol and $\Delta G^0_{VO} \approx -(360–400)$ kJ/mol, $C_{Zr}^{eq}(C_O^{eq})^2 \approx 1.5 \times 10^{-10}$ and $7 \times 10^{-8}$ for $T = 1000$ °C and 1700 °C are obtained, respectively. Such low values of the solubility of zirconium oxide in vanadium result from this compound having a considerably higher value of the formation energy than that for VO oxide, and point to its high stability up to the melting point of vanadium ($T_m = 1730$ °C). A similar specimen with

the oxygen concentration $C_O \approx 2.1$ at.% contains ≈0.2 at.% of oxygen in solid solution. According to Eq. (1), this results in a considerable (by a few orders) decrease of zirconium concentration in solid solution, and zirconium diffusion flow control of the coagulation rate of $ZrO_2$ particles.

It is evident from Fig. 2b that after annealing of Alloy 2 at $T = 1400$ °C, in conformity with the above considerations, the internally oxidized V–Cr–W–Zr specimen with a lower concentration of oxygen ($C_O \approx 1.2$ at.% after CTT-II) exhibits more pronounced (in contrast to CTT-I) recovery and recrystallization effects. The internally oxidized grain structure observed is inhomogeneous over the depth of the specimen. The grain size is as low as ≈20 μm in the surface layer of about 200 μm thickness with a higher content of the oxide phase (right part of Fig. 2b). This value is 5–6 times smaller than that in the specimens after annealing in the initial state (without the IO) (Fig. 2a). Approaching the central part of a 1-mm-thick specimen, the grain size gradually increases up to ≈50 μm.

After CTT-I ($C_O \approx 2.1$ at.%) in case of a higher volume fraction of the oxide-phase particles and a lower rate of their coagulation, an effective suppression of recrystallization at $T = 1400$ °C is observed throughout the whole thickness of the studied specimens (Fig. 2c). A large number of misoriented fragments with sizes less than 10 μm and the maze geometry of their boundaries indicate a complete suppression of collective recrystallization across the entire thickness of internally oxidized specimens.

It is clear that the effective stoppers suppressing grain-boundary migration are $ZrO_2$ particles possessing high thermal stability. It is evident in Fig. 2d that under conditions of coagulation at the annealing temperature, a two-phase structure becomes formed in the specimen with a widely varied distribution of the $ZrO_2$ particle size. The particles in the size range from a few tens to several hundreds of nanometers are predominant. They are relatively uniformly distributed over the bulk of the material and have either monoclinic or orthorhombic lattice.

Investigation of the microstructure of the internally oxidized specimens after heat treatments at much higher temperatures demonstrated that if the oxygen concentration exceeded the level required for formation of the $ZrO_2$ oxide of a stoichiometric composition ($C_O > 2C_{Zr}$), the temperature of collective recrystallization increased from ≈1300 °C (TMT-I) to $T \geq 1400$ °C (Fig. 2).

Table 1 shows the characteristics of short-term strength and plasticity of vanadium alloys after the HCT via different regimes. Let us single out the following results:

1. Maximum hardening effects (compared to TMT-I, more than a double increase in yield stress at room temperature and 60–90% increase at $T = 800$ °C) are achieved in the internally oxidized specimens with a higher content of oxygen (HCT-I, Table 1). This is the structural state with higher (compared to HCT-II) values of volume fraction, dispersity, and thermal stability of nanosized $ZrO_2$ particles.
2. Behavior of the plasticity as a function of treatment modes is in general consistent with the well-known trend of its decrease with an increase in the material strength. Nevertheless, even in cases of maximal hardening effects (HCT-I), the value of relative elongation of high-strength internally oxidized specimens at 20 °C remains quite high ($\delta \approx 12$ %).

**Table 1**
The effect of treatment modes on mechanical properties of vanadium alloys.

| The mode of treatment and oxygen concentration $C_O$ (at.%) | Testing temperature $T = 20$ °C | | Testing temperature $T = 800$ °C | |
|---|---|---|---|---|
| | $\sigma_{0.1}$ (MPa) | $\delta$ (%) | $\sigma_{0.1}$ (MPa) | $\delta$ (%) |
| Alloy 1 (V–Cr–Zr–C,N,O) | | | | |
| TMT-I | 230–250 | 23–26 | 170–200 | 24–27 |
| CTT-I, $C_O \approx 1.4$ | 575–590 | 10–13 | 325–340 | 7–9 |
| CTT-II, $C_O \approx 0.7$ | 410–425 | 18–22 | 240–270 | 10–13 |
| Alloy 2 (V–Cr–W–Zr–C,N,O) | | | | |
| TMT-I | 290–305 | 22–26 | 180–220 | 23–26 |
| CTT-I, $C_O \approx 2.1$ | 700–720 | 11–13 | 315–330 | 3–6 |
| CTT-II, $C_O \approx 1.2$ | 475–500 | 13–17 | 270–285 | 10–12 |

$\sigma_{0.1}$—yield strength, $\delta$—relative elongation to fracture.

Very high strengthening effects are achieved via two principal hardening mechanisms: dispersion hardening by nanosized $ZrO_2$ particles in addition with substructural hardening by the defect substructure elements (dislocations and different misorientation boundaries) pinned by these particles. According to [6], an important factor ensuring high efficiency of dispersion hardening with nanometric oxide particles is the impossibility of their destruction (interception) by glide dislocations and, as a result, the necessity of their by-passing via Orowan-type mechanism, which ensures an inverse dependence of Orowan stress on a particle's size [9,10].

We believe that the high thermal stability of these particles and defect substructure serve as a good indication of a promising application of the methods proposed here to improve not only the short-term but also the long-term high-temperature strength of vanadium alloys of V–Me(Cr, W)–Zr system.

To sum up, a critically important advantage of the dispersion hardening method, discussed in this study, is its possible implementation on the available semi-finished products or articles (such as sheets, foil rolls, pipes, etc.) produced from the initial high-technology and low-strength vanadium alloys.

## 5. Conclusion

In this study we investigated the features of the heterophase and defect substructure formation in vanadium alloys V–Cr–Zr (Alloy 1) and V–Cr–W–Zr (Alloy 2) as a function of the modes of their low-temperature diffusion-controlled doping with oxygen. We reported our methods and regimes of chemical–thermal treatments of these alloys (CTT-I, CTT-II), which ensure their diffusion doping with oxygen, followed by formation of the nanosized $ZrO_2$ particles of controllable dispersity.

It has been found out that thermal stability of the nanosized heterophase and defect structure of internally oxidized specimens is determined by the zirconium-to-oxygen concentration ratio in these alloys. For the oxygen concentrations in the internally oxidized specimens exceeding that required for a stoichiometric ($C_O > 2C_{Zr}$) $ZrO_2$ oxide to be formed, the temperature of collective recrystallization could be increased from ≈1300 °C to ≥1400 °C.

The treatment regimes proposed in this study ensure higher effects of dispersion and substructured hardening of a material: a two-fold increase in the yield stress at room temperature and its increase by 60–90 % at $T = 800$ °C.

## Acknowledgments

This work was sponsored by the State Atomic Energy Corporation ROSATOM under government contract no. H.4x.44.90.13.1082 with A.A. Bochvar High Technology Research Institute of Inorganic Materials with a partial support of Tomsk State University Competitiveness Improvement Program.

## References

[1] R.J. Kurtz R.J., K. Abe, V.M. Chernov, V.A. Kazakov, G.E. Lucas, H. Matsui, T. Muroga, G.R. Odette, D.L. Smith, S.J. Zinkle, J. Nucl. Mater. 283–287 (2000) 70–78.
[2] V.M. Chernov, M.V. Leonteva-Smirnova, M.M. Potapenko, N.I. Budylkin, Yu.N. Devyatko, A.G. Ioltoukhovskiy, E.G. Mironova, A.K. Shikov, A.B. Sivak, G.N. Yermolaev, A.N. Kalashnikov, B.V. Kuteev, A.I. Blokhin, N.I. Loginov, V.A. Romanov, V.A. Belyakov, I.R. Kirillov, T.M. Bulanova, V.N. Golovanov, V.K. Shamardin, Yu.S. Strebkov, A.N. Tyumentsev, B.K. Kardashev, O.V. Mishin, B.A. Vasiliev, Nucl. Fusion 47 (2007) 839–848.
[3] T. Muroga, Compr. Nucl. Mater. 4-12 (2012) 391–406.

[4] M. Le Flem, J.-M. Gentzbittel, P. Wident, J. Nucl. Mater. 442 (Suppl. 1) (2013) S325–S329.
[5] A.N. Tyumentsev, I.A. Ditenberg, K.V. Grinyaev, I.V. Smirnov, Yu.P. Pinzhin, V.M. Chernov, M.M. Potapenko, V.A. Drobyshev, M.V. Kravtsova, Voprosy Atomnoi Nauki i Techniki, Seriya Termoyaderny Sintez 37 (1) (2014) 18–26; (Problems of Atomic Science and Technology Series Thermonuclear Fusion). http://vant.iterru.ru/engvant_2014_1/3.pdf.
[6] A.D. Korotaev, A.N. Tyumentsev, V.F. Sukhovarov, Dispersion Hardening of Heat-Resistant Metals (in Russian), Nauka, Siberian Branch, Novosibirsk, 1989.
[7] A.N. Tyumentsev, A.D. Korotaev, Yu.P. Pinzhin, S.V. Ovchinnikov, V.M. Chernov, M.M. Potapenko, J. Nucl. Mater. 367–370 (2007) 853–857.
[8] A.N. Tyumentsev, A.D. Korotaev, Yu.P. Pinzhin, I.A. Ditenberg, S.V. Litovchenko, V.M. Chernov, M.M. Potapenko, J. Nucl. Mater. 329–333 (2004) 429–433.
[9] E. Orowan, Symposium on Internal Stresses in Metals and Alloys, Institute of Metals, 1948, p. 451.
[10] A. Kelly, R.B. Nicholson, Precipitation Hardening, A Pergamon Press Book, The Macmillan Company, New York, 1963, p. 300.